

SPARSE SELF-CALIBRATION BY MAP METHOD FOR MIMO RADAR IMAGING

Changchang Liu, Jin Yan, Weidong Chen

Department of Electronic Engineering and Information Science
University of Science and Technology of China, Hefei, Anhui, P.R. China
Email:cccliu@mail.ustc.edu.cn, yjin08@mail.ustc.edu.cn, wdchen@ustc.edu.cn.

ABSTRACT

Multiple-input multiple-output (MIMO) radar is expected to achieve good inversion performance by utilizing space diversity technology. However, traditional imaging methods often fail owing to the practical constraints that the available transmitters and receivers are very few and the number of snapshots is very limited. More seriously, the unavoidable position errors of the transmitters and the receivers would further deteriorate the imaging results. In this paper, by exploiting the sparse priority of the target, the sparse self-calibration by maximum a posterior probability method (SSC-MAP) is proposed to provide high resolution image and realize accurate position calibration at the same time. Numerical simulations verify the effectiveness of the proposed method.

Index Terms— MIMO radar imaging, MAP method, sparse inversion, self-calibration.

1. INTRODUCTION

Recently, multiple-input multiple-output (MIMO) radar has been shown to have the potential to achieve high resolution imaging performance through space diversity [1][2]. For MIMO radar, multiple antennas simultaneously transmit different waveforms and multiple antennas receive the signals reflected from the target at different aspect angles. Therefore, compared with traditional radar schemes, MIMO radar can obtain more spatial samplings of the target, which directly leads to better inversion performance.

Considering the practical complications, the number of transmitters and receivers is frequently restricted by the system complexity and the snapshots are constrained by the limited imaging time. So most existing methods can not provide good imaging results for MIMO radar system. Nonetheless, in most radar imaging applications especially the spaceborne/airborne applications, the scatterers of the targets are often distributed sparsely, i.e. the number of actual scatterers is much smaller than that of the potential scatterers. Hence, by exploiting the sparse priority more accurate target description can be obtained by sparse recovery technique [3].

The work in this paper is supported by National Natural Science Foundation of China under Grant No. 61172155.

Furthermore, the position errors of the transmitters and the receivers are likely to exist in practical applications. This problem, if not taken seriously, would greatly affect the imaging performance. Various calibration methods have been developed in the literature for direction of arrival (DOA) estimation [4][5] while few research is related to MIMO radar imaging. Herein we combine the sparse recovery technique and the self-calibration technique to develop the sparse self-calibration by maximum a posterior probability method (SSC-MAP). Moreover, according to [3], we adopt the self-adaptive parameter estimation operation in our method to avoid the complex parameter-choosing process. Therefore, our SSC-MAP method alternatively iterates among sparse reconstruction, self calibration and parameter update.

The outline of this paper is as follows. Section II establishes the imaging model for MIMO radar system with position errors. Section III describes the SSC-MAP method in detail. Section IV briefly discusses the convergence and the initialization of the algorithm, and presents several examples to illustrate the performance of the proposed algorithm.

2. MODEL ESTABLISHMENT

Consider a narrowband colocated MIMO radar system with M transmitters and N receivers as described in [2]. Let $\mathbf{s}_m = (s_m(1) \dots s_m(L))^T$ represent the transmitted waveform for the m^{th} ($m = 1 \dots M$) transmitter [3]. We collect the set of the transmitted waveforms $\{\mathbf{s}_m\}_{m=1}^M$ into a matrix $\mathbf{s} = (\mathbf{s}_1 \dots \mathbf{s}_M)^T$. Assuming there are U range bins and V angular bins in the scene of interest, \mathbf{S} refers to the zero-appended waveform matrix considering the shift in sampling intervals,

$$\mathbf{S} = [\mathbf{s} \quad \mathbf{0}_{M \times (U-1)}]_{M \times (L+U-1)}. \quad (1)$$

As $\{\theta_v\}_{v=1}^V$ divides the scene, the transmitting and receiving steering vectors, for the v^{th} angular bin, are denoted by \mathbf{a}_v and \mathbf{b}_v , respectively. Considering a special configuration that a uniform linear array is used for both the transmitters and the receivers where the first transmitter and the first receiver are assumed to be placed at the same position, the steering vectors can be written as

$$\mathbf{a}_v = \left(1 \quad e^{-\frac{j2\pi\Delta_t \sin \theta_v}{\lambda_0}} \quad \dots \quad e^{-\frac{j2\pi(M-1)\Delta_t \sin \theta_v}{\lambda_0}} \right)^T, \quad (2)$$

$$\mathbf{b}_v = \left(1 \ e^{-\frac{j2\pi\Delta_r \sin \theta_v}{\lambda_0}} \ \dots \ e^{-\frac{j2\pi(N-1)\Delta_r \sin \theta_v}{\lambda_0}} \right)^T, \quad (3)$$

where Δ_t and Δ_r represent the inter-element spacing of the transmitting array and the receiving array respectively, and λ_0 is the carrier wavelength of the system.

We let $\{x_{u,v}\}_{u=1,v=1}^{U,V}$ denote the complex reflection coefficient of each bin in the scene of interest. The received echo matrix \mathbf{Y} can be written as

$$\mathbf{Y} = \sum_{u=1}^U \sum_{v=1}^V x_{u,v} \mathbf{b}_v \mathbf{a}_v^T \mathbf{S} \mathbf{J}_u + \mathbf{E}, \quad (4)$$

where \mathbf{E} denotes the additive noise matrix and \mathbf{J}_u represents the shift matrix designed to describe the reflected waveform from different range bin, and is defined by

$$\mathbf{J}_u = \begin{pmatrix} \overbrace{0 \dots 0}^u & & 0 \\ & \ddots & \\ & & 1 \\ 0 & & & 0 \end{pmatrix}_{(L+U-1) \times (L+U-1)}.$$

To represent the received signal in its vector form, we define $\mathbf{y} = \text{vec}(\mathbf{Y})$, $\mathbf{e} = \text{vec}(\mathbf{E})$ and $\mathbf{h}_{u,v} = \text{vec}(\mathbf{b}_v \mathbf{a}_v^T \mathbf{S} \mathbf{J}_u)$. Moreover, we let

$$\begin{aligned} \mathbf{H} &= (\mathbf{h}_{1,1} \ \mathbf{h}_{1,2} \ \dots \ \mathbf{h}_{U,V}), \\ \mathbf{x} &= (x_{1,1} \ x_{1,2} \ \dots \ x_{U,V})^T. \end{aligned} \quad (5)$$

In this way, the received signal can be redefined as

$$\mathbf{y} = \mathbf{H} \mathbf{x} + \mathbf{e}. \quad (6)$$

Taking the practical constraints into consideration, (6) is always an underdetermined function by which good inverse performance can not be achieved without enough prior knowledge. For most spaceborne/airborne target, the sparse priority can be utilized for MIMO radar high-resolution imaging with limited measurements.

For practical application, supposing that the position errors of the transmitters and the receivers are $\{dt_m\}_{m=1}^M$ and $\{dr_n\}_{n=1}^N$ respectively, the steering vectors can be transformed into

$$\begin{aligned} \mathbf{a}'_v &= \left(e^{-\frac{j2\pi dt_1 \sin \theta_v}{\lambda_0}} \ \dots \ e^{-\frac{j2\pi((M-1)\Delta_t + dt_M) \sin \theta_v}{\lambda_0}} \right)^T, \\ \mathbf{b}'_v &= \left(e^{-\frac{j2\pi dr_1 \sin \theta_v}{\lambda_0}} \ \dots \ e^{-\frac{j2\pi((M-1)\Delta_r + dr_M) \sin \theta_v}{\lambda_0}} \right)^T. \end{aligned} \quad (7)$$

Considering that the position errors are rather small, we can make the following approximation

$$\begin{aligned} e^{-\frac{j2\pi dt_m \sin \theta_v}{\lambda_0}} &\approx 1 - \frac{j2\pi dt_m \sin \theta_v}{\lambda_0}, \quad m = 1, 2, \dots, M, \\ e^{-\frac{j2\pi dr_n \sin \theta_v}{\lambda_0}} &\approx 1 - \frac{j2\pi dr_n \sin \theta_v}{\lambda_0}, \quad n = 1, 2, \dots, N. \end{aligned} \quad (8)$$

Next, we define the transmitting error vector Λ_v^t and the receiving error vector Λ_v^r , for v^{th} angular bin, as following

$$\begin{aligned} \Lambda_v^t &= (\Lambda_{v1}^t \ \Lambda_{v2}^t \ \dots \ \Lambda_{vM}^t)^T, \\ \Lambda_v^r &= (\Lambda_{v1}^r \ \Lambda_{v2}^r \ \dots \ \Lambda_{vN}^r)^T, \end{aligned} \quad (9)$$

where

$$\begin{aligned} \Lambda_{vm}^t &= -\frac{j2\pi dt_m \sin \theta_v}{\lambda_0} e^{-\frac{j2\pi(m-1)\Delta_t \sin \theta_v}{\lambda_0}}, \\ \Lambda_{vn}^r &= -\frac{j2\pi dr_n \sin \theta_v}{\lambda_0} e^{-\frac{j2\pi(n-1)\Delta_r \sin \theta_v}{\lambda_0}}. \end{aligned} \quad (10)$$

So the received signal with position errors can be written as

$$\mathbf{Y} = \sum_{u=1}^U \sum_{v=1}^V x_{u,v} \mathbf{b}'_v \mathbf{a}'_v{}^T \mathbf{S} \mathbf{J}_u + \mathbf{E}, \quad (11)$$

where $\mathbf{b}'_v \mathbf{a}'_v{}^T = \mathbf{b}_v \mathbf{a}_v^T + \mathbf{b}_v \Lambda_v^{tT} + \Lambda_v^r \mathbf{a}_v^T + \Lambda_v^r \Lambda_v^{tT}$. Further ignoring the product of Λ_v^r and Λ_v^{tT} yields

$$\mathbf{b}'_v \mathbf{a}'_v{}^T \approx \mathbf{b}_v \mathbf{a}_v^T + \mathbf{b}_v \Lambda_v^{tT} + \Lambda_v^r \mathbf{a}_v^T. \quad (12)$$

Similar to (6), the received signal can be redefined as

$$\mathbf{y} = (\mathbf{H} + \Phi^t + \Phi^r) \mathbf{x} + \mathbf{e}, \quad (13)$$

where

$$\begin{aligned} \Phi^t &= (\varphi_{1,1}^t \ \dots \ \varphi_{U,V}^t), \quad \varphi_{u,v}^t = \text{vec}(\mathbf{b}_v \Lambda_v^{tT} \mathbf{S} \mathbf{J}_u), \\ \Phi^r &= (\varphi_{1,1}^r \ \dots \ \varphi_{U,V}^r), \quad \varphi_{u,v}^r = \text{vec}(\Lambda_v^r \mathbf{a}_v^T \mathbf{S} \mathbf{J}_u). \end{aligned} \quad (14)$$

3. SSC-MAP ALGORITHM

Suppose that every potential scatterer $\{x_{u,v}\}_{u=1,v=1}^{U,V}$ exploits sparsity with laplace prior $p(x_{u,v}) = e^{-|x_{u,v}|}$ [6]. Hence, \mathbf{x} satisfies

$$p(\mathbf{x}) = \exp\{-\|\mathbf{x}\|_1\}. \quad (15)$$

Assume that the position error of every transmitter and every receiver is independent from each other and satisfies

$$\{dt_m\}_{m=1}^M \sim \mathcal{N}(0, \xi_t), \quad \{dr_n\}_{n=1}^N \sim \mathcal{N}(0, \xi_r). \quad (16)$$

Defining η as the noise power, we assume

$$\mathbf{y} | \{dt_m, dr_n\}_{m=1,n=1}^{M,N}, \mathbf{x}, \eta \sim \mathcal{CN}((\mathbf{H} + \Phi^t + \Phi^r) \mathbf{x}, \eta \mathbf{I}). \quad (17)$$

We can estimate \mathbf{x} , $\{dt_m\}_{m=1}^M$, $\{dr_n\}_{n=1}^N$, η , ξ_t and ξ_r via MAP method which maximizes

$$\begin{aligned} &p(\mathbf{x}, \{dt_m, dr_n\}_{m=1,n=1}^{M,N}, \eta, \xi_t, \xi_r | \mathbf{y}) \\ &\propto p(\mathbf{x}) p(\{dt_m\}_{m=1}^M) p(\{dr_n\}_{n=1}^N) \\ &\cdot p(\mathbf{y} | \{dt_m, dr_n\}_{m=1,n=1}^{M,N}, \mathbf{x}, \eta) p(\eta) p(\xi_t) p(\xi_r) \end{aligned} \quad (18)$$

Assuming $p(\eta) \propto 1$, $p(\xi_t) \propto 1$, $p(\xi_r) \propto 1$ and combining with (15)(16)(17), then (18) can be expanded as

$$\begin{aligned} &p(\mathbf{x}, \{dt_m, dr_n\}_{m=1,n=1}^{M,N}, \xi_t, \xi_r, \eta | \mathbf{y}) \propto \exp\{-\|\mathbf{x}\|_1\} \\ &\cdot \prod_{m=1}^M \frac{1}{\sqrt{2\pi\xi_t}} \exp\left\{-\frac{dt_m^2}{2\xi_t}\right\} \prod_{n=1}^N \frac{1}{\sqrt{2\pi\xi_r}} \exp\left\{-\frac{dr_n^2}{2\xi_r}\right\} \\ &\cdot \frac{1}{(\pi\eta)^{N(L+U-1)}} \exp\left\{-\frac{\|\mathbf{y} - (\mathbf{H} + \Phi^t + \Phi^r) \mathbf{x}\|_2^2}{\eta}\right\}. \end{aligned} \quad (19)$$

Taking the negative logarithm operation to (19), we get the following cost function

$$F = \|\mathbf{x}\|_1 + \frac{M}{2} \ln \xi_t + \frac{N}{2} \ln \xi_r + \sum_{m=1}^M \frac{dt_m^2}{2\xi_t} + \sum_{n=1}^N \frac{dr_n^2}{2\xi_r} + N(L+U-1) \ln \eta + \frac{1}{\eta} \|\mathbf{y} - (\mathbf{H} + \Phi^t + \Phi^r)\mathbf{x}\|_2^2. \quad (20)$$

The MAP method equivalently results in the minimization of F with respect to $\mathbf{x}, \{dt_m, dr_n\}_{m=1, n=1}^{M, N}, \xi_t, \xi_r, \eta$, which is a nonlinear problem. According to [4], we adopt an alternately iterative method. Defining k as the iteration index, we optimize \mathbf{x}_{k+1} with $\{dt_{mk}, dr_{nk}\}_{m=1, n=1}^{M, N}, \eta_k, \xi_{tk}, \xi_{rk}$ fixed and then optimize $\{dt_{m(k+1)}, dr_{n(k+1)}\}_{m=1, n=1}^{M, N}$ with $\mathbf{x}_{k+1}, \eta_k, \xi_{tk}, \xi_{rk}$ fixed. Then, the parameters $\eta_{k+1}, \xi_{t(k+1)}, \xi_{r(k+1)}$ are updated at each iteration. Detailed algorithm is stated as follows.

3.1. Sparse Reconstruction

Supposing that $\{dt_{mk}, dr_{nk}\}_{m=1, n=1}^{M, N}$ are known and then defining $\Gamma_k = \mathbf{H} + \Phi_k^t + \Phi_k^r$, we try to find the optimal \mathbf{x}_{k+1} to minimize the following equivalent cost function.

$$F_1 = \|\mathbf{y} - \Gamma_k \mathbf{x}_{k+1}\|_2^2 + \eta_k \|\mathbf{x}_{k+1}\|_1. \quad (21)$$

This typical ℓ_1 regularization least square problem can be reformulated as optimizing $\mathbf{p}_{k+1}, \mathbf{q}_{k+1}, \boldsymbol{\rho}_{k+1}$ to

$$\begin{cases} \min \left\| \tilde{\Gamma}_k \begin{pmatrix} \mathbf{p}_{k+1} \\ \mathbf{q}_{k+1} \end{pmatrix} - \tilde{\mathbf{y}} \right\|_2^2 + \eta_k \mathbf{1}^T \boldsymbol{\rho}_{k+1}, \\ \text{s.t. } \left(p_{u,v(k+1)}^2 + q_{u,v(k+1)}^2 \right)^{\frac{1}{2}} \leq \rho_{u,v(k+1)}. \end{cases} \quad (22)$$

where $\mathbf{p}_{k+1} = \text{Re}(\mathbf{x}_{k+1}), \mathbf{q}_{k+1} = \text{Im}(\mathbf{x}_{k+1})$.

$$\tilde{\Gamma}_k = \begin{pmatrix} \text{Re}(\Gamma_k) & -\text{Im}(\Gamma_k) \\ \text{Im}(\Gamma_k) & \text{Re}(\Gamma_k) \end{pmatrix}, \quad \tilde{\mathbf{y}} = \begin{pmatrix} \text{Re}(\mathbf{y}) \\ \text{Im}(\mathbf{y}) \end{pmatrix} \quad (23)$$

Here we use the truncated Newton interior-point method [7] to solve (25), which is proved to have good balance between convergent performance and computer complexity.

3.2. Self Calibration

Next, we use \mathbf{x}_{k+1} to estimate $\{dt_{m(k+1)}, dr_{n(k+1)}\}_{m=1, n=1}^{M, N}$. Denoting $\gamma_{tk} = \eta_k/2\xi_{tk}, \gamma_{rk} = \eta_k/2\xi_{rk}$, the cost function can be simplified as

$$F_2 = \|\mathbf{y} - \Gamma_{k+1} \mathbf{x}_{k+1}\|_2^2 + \gamma_{tk} \sum_{m=1}^M dt_{m(k+1)}^2 + \gamma_{rk} \sum_{n=1}^N dr_{n(k+1)}^2. \quad (24)$$

In (24), considering that the transmitters and the receivers are independent from each other, we calibrate every position error of the transmitter and the receiver respectively. For the m^{th} transmitter, we optimize $dt_{m(k+1)}$ to

$$\begin{cases} \min \|z_k^{tm} - \Phi_k^{tm} dt_{m(k+1)} \mathbf{x}_{k+1}\|_2^2 + \gamma_{tk} dt_{m(k+1)}^2 \\ \text{s.t. } dt_{m(k+1)} \text{ is real.} \end{cases} \quad (25)$$

where Φ_k^{tm} is the corresponding Φ_k^t with $dt_{\tilde{m}} = \delta(\tilde{m} - m)$, $z_k^{tm} = \mathbf{y} - \left(\mathbf{H} + \Phi_k^r + \sum_{i=1}^{m-1} \Phi_k^{ti} dt_{i(k+1)} \right) \mathbf{x}_{k+1}$. We get

$$dt_{m(k+1)} = \frac{\text{Re} \left((\Phi_k^{tm} \mathbf{x}_{k+1})^H z_k^{tm} \right)}{\text{Re} \left((\Phi_k^{tm} \mathbf{x}_{k+1})^H \Phi_k^{tm} \mathbf{x}_{k+1} \right) + \gamma_{tk}}. \quad (26)$$

After taking the operation above for every transmitter to obtain $\{dt_{m(k+1)}\}_{m=1}^M$, we can get Φ_{k+1}^t according to (10)(14). Similarly, for the n^{th} receiver, we expect to find the optimal $dr_{n(k+1)}$ to

$$\begin{cases} \min \|z_k^{rn} - \Phi_k^{rn} dr_{n(k+1)} \mathbf{x}_{k+1}\|_2^2 + \gamma_{rk} dr_{n(k+1)}^2 \\ \text{s.t. } dr_{n(k+1)} \text{ is real.} \end{cases} \quad (27)$$

where Φ_k^{rn} is the corresponding Φ_k^r with $dr_{\tilde{n}} = \delta(\tilde{n} - n)$, $z_k^{rn} = \mathbf{y} - \left(\mathbf{H} + \Phi_{k+1}^t + \sum_{j=1}^{n-1} \Phi_k^{rj} dr_{j(k+1)} \right) \mathbf{x}_{k+1}$. Then, we find the optimal solution as

$$dr_{n(k+1)} = \frac{\text{Re} \left((\Phi_k^{rn} \mathbf{x}_{k+1})^H z_k^{rn} \right)}{\text{Re} \left((\Phi_k^{rn} \mathbf{x}_{k+1})^H \Phi_k^{rn} \mathbf{x}_{k+1} \right) + \gamma_{rk}}. \quad (28)$$

In a similar way, we can update Φ_{k+1}^r from $\{dr_{n(k+1)}\}_{n=1}^N$.

3.3. Parameter Update

To avoid the complex criteria for parameter estimation [8], here we propose a self-adaptive parameter updating method to dynamically determine $\eta_{k+1}, \xi_{t(k+1)}, \xi_{r(k+1)}$. Setting $\partial F / \partial \eta_{k+1} = 0$ leads to

$$\eta_{k+1} = \frac{\|\mathbf{y} - (\mathbf{H} + \Phi_{k+1}^t + \Phi_{k+1}^r) \mathbf{x}_{k+1}\|_2^2}{N(L+U-1)}. \quad (29)$$

Similarly, letting $\partial F / \partial \xi_{t(k+1)} = \partial F / \partial \xi_{r(k+1)} = 0$, we get

$$\xi_{t(k+1)} = \frac{1}{M} \sum_{m=1}^M dt_{m(k+1)}^2, \quad \xi_{r(k+1)} = \frac{1}{N} \sum_{n=1}^N dr_{n(k+1)}^2. \quad (30)$$

We set $k \leftarrow k+1$ and repeat the three steps above until SSC-MAP shows no obvious improvement.

4. NUMERICAL SIMULATIONS

Considering the convexity of F_1 , the interior method shows good convergent performance [7]. Besides, $\{dt_{m(k+1)}\}_{m=1}^M, \{dr_{n(k+1)}\}_{n=1}^N$ and $\eta_{k+1}, \xi_{t(k+1)}, \xi_{r(k+1)}$ are all closed form solutions to the minimization of the cost function F . Hence the value of F keeps decreasing as k increases. However, a key guarantee for the convergence to a good solution is the initialization of the algorithm. Here we initialize \mathbf{x} by applying matched filter (MF).

$$\mathbf{x}_{u,v(0)} = (\mathbf{h}_{u,v}^H \mathbf{h}_{u,v})^{-1} \mathbf{h}_{u,v}^H \mathbf{y}. \quad (31)$$

Assuming $\{dt_{m(0)}\}_{m=1}^M = \{dr_{n(0)}\}_{n=1}^N = 0$, thus $\eta_0, \xi_{t(0)}$ and $\xi_{r(0)}$ can be obtained according to (29)(30).

In order to test the performance of SSC-MAP, we consider a system with $M = 5$ transmitters, $N = 5$ receivers and the

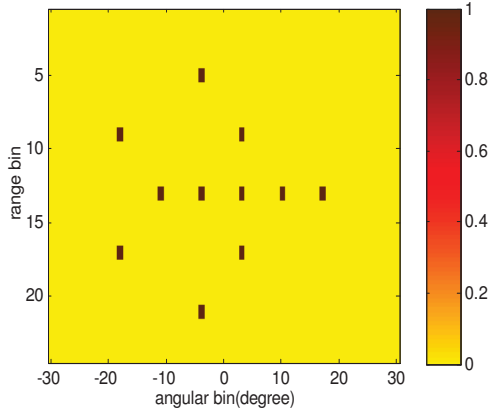


Fig. 1. Scatterer distribution of the target.

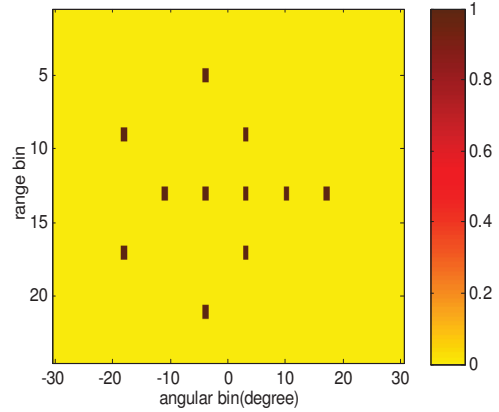


Fig. 3. Imaging result via SSC-MAP.

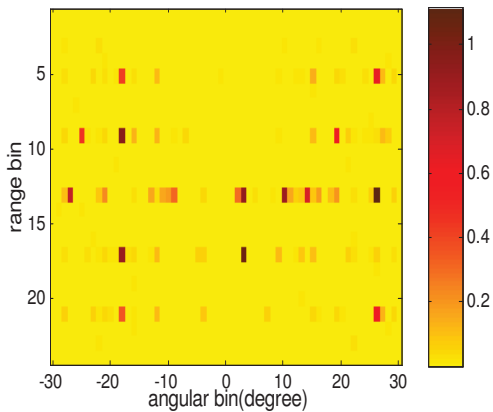


Fig. 2. Imaging result without calibration.

number of snapshots $L = 63$. The transmitters and the receivers are expected to be uniformly positioned with spacings of 2.5λ and 0.5λ , respectively. We set $\xi_t = (0.1\lambda)^2$, $\xi_r = (0.02\lambda)^2$ and the signal-to-noise ratio (SNR) to 10dB.

We provide the original scatterer distribution of the target in Fig. 1. There are $U = 24$ bins in the range direction and $V = 63$ bins in the angular direction. And there are 11 scatterers with unit reflection coefficient in the scene of interest.

Fig. 2 shows the inversion performance without calibration, which is noticeably poor because of the position errors.

Fig. 3 represents the imaging result via SSC-MAP method. As expected, the new method can achieve better reconstruction performance with accurate self calibration ability.

5. CONCLUSIONS

We present the SSC-MAP method to realize high resolution imaging and self-calibrating the position errors for MIMO radar system. The derivations and numerical examples illus-

trate the effectiveness of the new method, which shows the potential for the method to be applied in practical system.

References

- [1] E. Fishler, A. Haimovich, R. Blum, D. Chizhik, L. Cimini, and R. Valenzuela, "Mimo radar: An idea whose time has come," in *Radar Conference, 2004. Proceedings of the IEEE*. IEEE, 2004, pp. 71–78.
- [2] J. Li and P. Stoica, "Mimo radar diversity means superiority," *MIMO Radar Signal Processing*, pp. 1–64, 2007.
- [3] X. Tan, W. Roberts, J. Li, and P. Stoica, "Sparse learning via iterative minimization with application to mimo radar imaging," *Signal Processing, IEEE Transactions on*, no. 99, pp. 1–1, 2011.
- [4] A.J. Weiss and B. Friedlander, "Array shape calibration using sources in unknown locations—a maximum likelihood approach," *Acoustics, Speech and Signal Processing, IEEE Transactions on*, vol. 37, no. 12, pp. 1958–1966, 1989.
- [5] A. Ferreol, P. Larzabal, and M. Viberg, "On the asymptotic performance analysis of subspace doa estimation in the presence of modeling errors: Case of music," *Signal Processing, IEEE Transactions on*, vol. 54, no. 3, pp. 907–920, 2006.
- [6] S.D. Babacan, R. Molina, and A.K. Katsaggelos, "Bayesian compressive sensing using laplace priors," *Image Processing, IEEE Transactions on*, vol. 19, no. 1, pp. 53–63, 2010.
- [7] S.J. Kim, K. Koh, M. Lustig, S. Boyd, and D. Gorinevsky, "An interior-point method for large-scale l1-regularized least squares," *Selected Topics in Signal Processing, IEEE Journal of*, vol. 1, no. 4, pp. 606–617, 2007.
- [8] L. Reichel and H. Sadok, "A new l-curve for ill-posed problems," *Journal of Computational and Applied Mathematics*, vol. 219, no. 2, pp. 493–508, 2008.